MALAYSIAN JOURNAL OF MICROSCOPY

Journal homepage: https://malaysianjournalofmicroscopy.org

RESEARCH ARTICLE

EFFECTS OF SINTERING TEMPERATURE ON THE MICROSTRUCTURES AND ADHESION STRENGTH OF SLURRY SPRAYED YSZ/NiCoCrAlYTa FUNCTIONALLY GRADED-THERMAL BARRIER COATING ON INCONEL 625

Fadzlun Nadrah Mohd Sharuddin[1], Muhamad Azizi Mat Yajid[1,2,*]

[1]Department of Materials, Manufacturing and Industrial Engineering, Faculty of Mechanical Engineering, Universiti Teknologi Malaysia, 81310 Skudai, Johor, Malaysia.
[2]Materials Research and Consultancy Group (MRCG), Faculty of Mechanical Engineering, Universiti Teknologi Malaysia, 81310, Skudai, Johor, Malaysia.

Abstract. Thermal barrier coating (TBC) has been widely used in protecting turbine components exposed to extreme temperature conditions. The conventional TBC system comprises of a metallic bond coat layer deposited on the substrate and yttria stabilized zirconia (YSZ) top layer. However, the thermal expansion mismatch between the bond coat and top coat layer has become a problem that leads to coating delamination. To mitigate this issue, the functionally graded-thermal barrier coating (FG-TBC) method is adopted, where a homogenous coating structure consists of composite materials layered on the substrate by gradually changing the compositional ratios over the coating thickness. This smooth transition from the substrate to the top layer minimizes the thermal expansion mismatch between the coating layers, reduces the internal residual stresses, and increases the bonding strength. On the other hand, plasma spray has been the commonly used method for depositing TBC. However, in this study, YSZ/NiCoCrAlYTa FG-TBC was fabricated by using the slurry spray technique (SST), considering the lower cost and simplicity of the method. In determining the optimum sintering temperature, effects of various sintering temperatures (i.e., 950, 1000, 1050, 1100, and 1150 ℃) on the microstructures and adhesion strength were investigated. Scanning electron microscopy (SEM) and energy dispersive spectroscopy (EDS) were applied to characterize the microstructures, and a pull-off adhesion test was conducted to measure the adhesion strength between the coating layers and the substrate. The findings showed that samples sintered at 1100 ℃ revealed dense FG-TBC layers with a continuous reaction layer at the substrate interface, minimal porosity, and no presence of cracks, with the highest adhesion strength, which is 22.87 MPa. Therefore, the effective sintering temperature for slurry-sprayed YSZ/NiCoCrAlYTa FG-TBC was considerably achieved at 1100 ℃.

Keywords: Thermal barrier coating, functionally graded coating, yttria stabilized zirconia, sintering temperature.

Article Info

Received 10 January 2026
Accepted 25 April 2026
Published 8 June 2026

***Corresponding author: azizi@utm.my**

ISSN: 1823-7010, eISSN: 2600-7444

1. INTRODUCTION

In the aviation sector, the thrust-to-weight ratio of an aero-engine is a critical factor to ensure the aircraft is stable and more dynamic. Higher temperature at the turbine inlet can produce a higher thrust-weight ratio and improve the efficiency in a significant way. Turbine blades are the critical component that are constantly subjected to extreme working temperature conditions. This intense temperature condition can cause thermal and mechanical stresses that lead to failure due to overheating, fatigue, corrosion, and oxidation [1,2]. In order to protect and maximize the thermo-mechanical properties of turbine blades, the use of thermal barrier coating (TBC) is vital for the longevity and performance of the turbine. The application of TBCs may be able to sustain a thermal gradient between the coating and the surface of the turbine blades, in view that thermal and mechanical stresses can be reduced.

Throughout the years, conventional TBCs, which consist of a top coat ceramic layer, bond coat layer, and thermally grown oxide (TGO) layer, have been proven to protect hot components from high working temperatures. However, as the turbine inlet air temperature continues to increase in order to enhance the efficiency of gas turbine systems, the conventional structure of thermal barrier coatings (TBCs) encounters significant challenges in maintaining its functional performance and structural integrity. During long-term service at severe working temperatures, conventional TBCs are susceptible to premature coating failure due to micro-cracks induced by residual stresses. Previous researchers reported that TGO, phase transformation, and cooling rate are the primary factors in the development of high residual stresses in the ceramic top coat [3,4]. Due to the intrinsic brittleness of TGO, coating failure commonly occurs at the interface between the TGO and the bond coat layer. During service, elevated working temperatures promote the growth of TGO layers, which lead to thermal expansion mismatch between the layers and result in the increasing residual stresses upon cooling. Therefore, functionally graded-thermal barrier coatings (FG-TBCs) were designed to overcome the limitations of the conventional coating system. FG-TBCs are non-homogeneous coatings typically made up of advanced composite materials in which mechanical, thermal, and tribological properties vary gradually along the coating thickness [5]. The smooth and continuous transition of properties along the coating thickness makes FG-TBCs more attractive and dominant than conventional composite materials, as it can mitigate residual stresses within the coating layers.

The commonly used top-coat for TBCs is yttria-stabilized zirconia (YSZ) owing to its excellent thermo-physical properties, including high melting temperature (~2700 °C), low thermal conductivity (2.1 - 2.9 W/mk^{-1}), thermal expansion coefficient (11.0 × 10^{-6} K^{-1}) that is well matched with the substrate, as well as high fracture toughness and relatively high strength and wear resistance [6,7]. YSZ TBC produced by plasma spray is known as a state-of-the-art TBC due to the dense coating structure, lower thermal conductivity, and high corrosion resistance. However, these conventional coating methods were reported to be expensive, complex, and associated with several technical limitations [8]. Coatings produced by plasma spraying were also discovered to exhibit shorter thermal-cycling life compared to other coating methods, such as electron beam physical vapor deposition (EB-PVD) [9,10]. This behavior is mainly attributed to the presence of segmented vertical cracks in the coating, which relieve thermal strain due to the thermal expansion mismatch between the coating and the substrate, thereby generating strain-tolerant plasma-sprayed coatings.

Hence, this study was focused on fabricating YSZ FG-TBC using a simple, flexible, and cost-effective method, namely the slurry spray technique (SST), which was expected to produce coatings with higher bonding strength and improved thermal shock resistance [11,12]. This technique utilizes relatively simple equipment, which can be operated manually or adapted to an automated system. Previous studies on TBCs produced by SST have demonstrated promising performances. Nguyen et al. [13] studied the thermal performance of YSZ/Ni FG-TBC produced by SST and found that the thermal conductivity was lower than that of coatings produced by air plasma spraying (APS). The difference could be explained by the higher porosity present in the coatings fabricated by SST. Therefore, in this study, the optimum sintering temperature for three-layered YSZ/NiCoCrAlYTa FG-TBC deposited by SST was determined by investigating its effects on coating microstructure and adhesion strength.

2. MATERIALS AND METHODS

2.1 Materials

A Ni-base superalloy, Inconel 625 (IN-625) from Baoji Tianbang Ti & Ni Co., China, with a composition of 59.8 % Ni, 22 % Cr, 9 % Mo, 4 % Fe, 4 % Ta, 0.4 % Si, 0.36 % Al, 0.34 % Ti, 0.08 % C, 0.01 % S, and 0.01 % P was used as the substrate. The raw materials used in this study included NiCoCrAlYTa powder from Oerlikon Metco, USA as the metal powder with composition of 28.99 % Ni, 22.03 % Al, 21.88 % Cr, 14.04 % Co, 9.66 % Y and 3.36 % Ta, and YSZ powder from Sigma-Aldrich, UK as the ceramic powder with composition of 67.51 % Zr, 8.32 % Y and 24.17 % O. Other coating materials included polyvinyl alcohol (PVA, from Sigma-Aldrich, UK) as a binder, tetrasodium pyrophosphate (TSPP, from Sigma-Aldrich, UK) as a dispersant material and distilled water as the solvent.

2.2 Substrate and slurry mixture preparation

The substrates were cut into 20 squares of 20 × 20 × 5 mm, and subsequently sand blasted using alumina abrasive grit (Mesh 36) to achieve an average surface roughness of >5 μm. Before coating deposition, the substrates were ultrasonically cleaned with acetone. For the preparation of the slurry mixture, the coating materials were first weighed according to their respective composition as depicted in Table 1. Distilled water was then agitated on a magnetic hot plate, followed by adding TSPP into the agitated solvent until fully dissolved. PVA was subsequently added gradually to minimize the risk of agglomeration. The mixture was continuously stirred at 100 ℃ for 30 min to ensure PVA's complete dissolution. Finally, NiCoCrAlYTa and YSZ powders were added to the solution to complete the preparation of the slurry mixture.

Table 1: Composition of the coating slurry materials

Coating material	Composition [wt%]
NiCoCrAlYTa +YSZ powder	46.0
PVA	2.5
TSPP	0.5
Distilled water	51.0

2.3 Coating fabrication

The slurry mixture was deposited onto the substrate using an Anest Iwata RG-3L gravity-feed spray gun. The distance between the spray gun nozzle and the substrate surface was controlled in a range of 100 to 150 mm to maintain fine atomization and prevent localized deposition of coating particles during coating deposition. The coated substrates were allowed to dry under ambient conditions for 3 h before the subsequent layers were deposited.

In this study, three functionally graded layers were fabricated, achieving a total coating layer thickness of 250 to 300 μm, which was considered the optimum thickness to prevent the formation of surface cracks. The graded composition of YSZ/NiCoCrAlYTa for each layer is shown in Figure 1. The green-coated samples were then subjected to pressure stamping, which is like powder compaction in powder metallurgy, with approximately 30 MPa compressive pressure. This step is crucial in SST to promote densification and improve adhesion strength. Prior to sintering, the coated samples underwent a binder burn-out (de-binding) process, in which the green coatings were heated at 500 ℃ for 2 h to ensure complete removal of PVA. Sintering was subsequently started by raising the furnace temperature up to the selected sintering temperatures (950, 1000, 1050, 1100, and 1150 ℃) and holding for 2 h. After sintering, the coated samples were allowed to cool to room temperature inside the furnace. According to our preliminary test, samples sintered at temperatures higher than 1150 ℃ resulted in

coating spallation. Therefore, the maximum sintering temperature in this study was pre-determined to be 1150 °C.

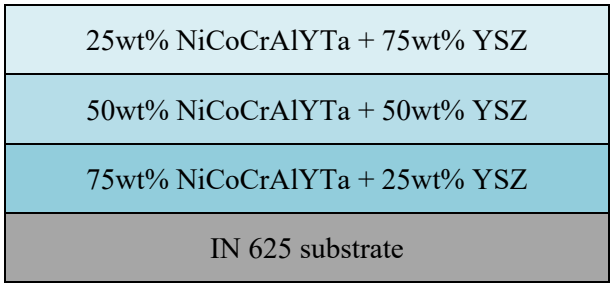

Figure 1: Yttria stabilized zirconia functionally-graded structure with bond coat-rich first layer, equivalent metal-ceramic second layer, and ceramic-rich third layer

2.4 Microstructural characterization

Detailed characterization of the coated samples was carried out to analyze the microstructural effects at different sintering temperatures. Surface and cross-sectional analyses were conducted using a variable-pressure scanning electron microscope (VPSEM, Hitachi S-3400N) equipped with an energy dispersive X-ray spectroscope (EDX). Prior to cross-sectional SEM observation, the samples were subjected to grinding and polishing to attain mirror-like surface finishing.

2.5 Mechanical evaluation

In this work, the adhesion strength between the graded coating layers and the substrate was evaluated using the pull-off adhesion testing method in accordance with ASTM D4541 standard. A portable and hand-operated PosiTest tester (DeFelsko Corporation, USA) was used to conduct the adhesion test. The device applied hydraulic pressure to measure the force required to detach the coating from its substrate, which represents the coating adhesion strength. A 10 mm-diameter dolly was used in this study, considering the 20 × 20 mm surface area of the coated sample. First and foremost, the base of the dolly and coating surface were cleaned and abraded to remove any contaminants. Then, epoxy adhesive Araldite, consisting of a two-part component (epoxy and hardener), was used to bond the dolly to the coated surface. The two components were mixed in a 1:1 ratio and applied to the base of the dolly. To ensure effective curing, the bonded samples were allowed to dry for 90 min at room temperature. Then, the actuator assembly was carefully connected to the head of the dolly and ensured that it was completely engaged. A moderate pull rate (1.0 MPa) was set in order to avoid shock loading during the test. Tensile load was then applied gradually to the dolly until failure occurred. Each test was repeated three times, and the average adhesion strength was recorded.

3. RESULTS AND DISCUSSION

3.1 Microstructures of coating layers at various sintering temperatures

Figure 2 shows the cross-sectional microstructure of samples sintered at 950, 1000, 1050, 1100, and 1150 °C, denoted as S950, S1000, S1050, S1100, and S1150, respectively. It can be observed that NiCoCrAlYTa and YSZ particles were distributed along the coating thickness according to their compositional ratio (Figure 1), exhibiting a gradual transition from the dense metallic region (NiCoCrAlYTa) region near the substrate to the ceramic-rich (YSZ) upper layer of the FG-TBC structure. Furthermore, the cross-sectional microstructures revealed consistently deposited FG-TBC layers as the coating thickness ranges between 276 and 283 μm, indicating good repeatability and stability during slurry spray deposition. The measured thicknesses were also within the range of the

effective thickness of TBCs produced by SST [14]. In addition, the images depict a dense coating layer with low porosity due to the adequate pressure applied during the pressure-stamping process.

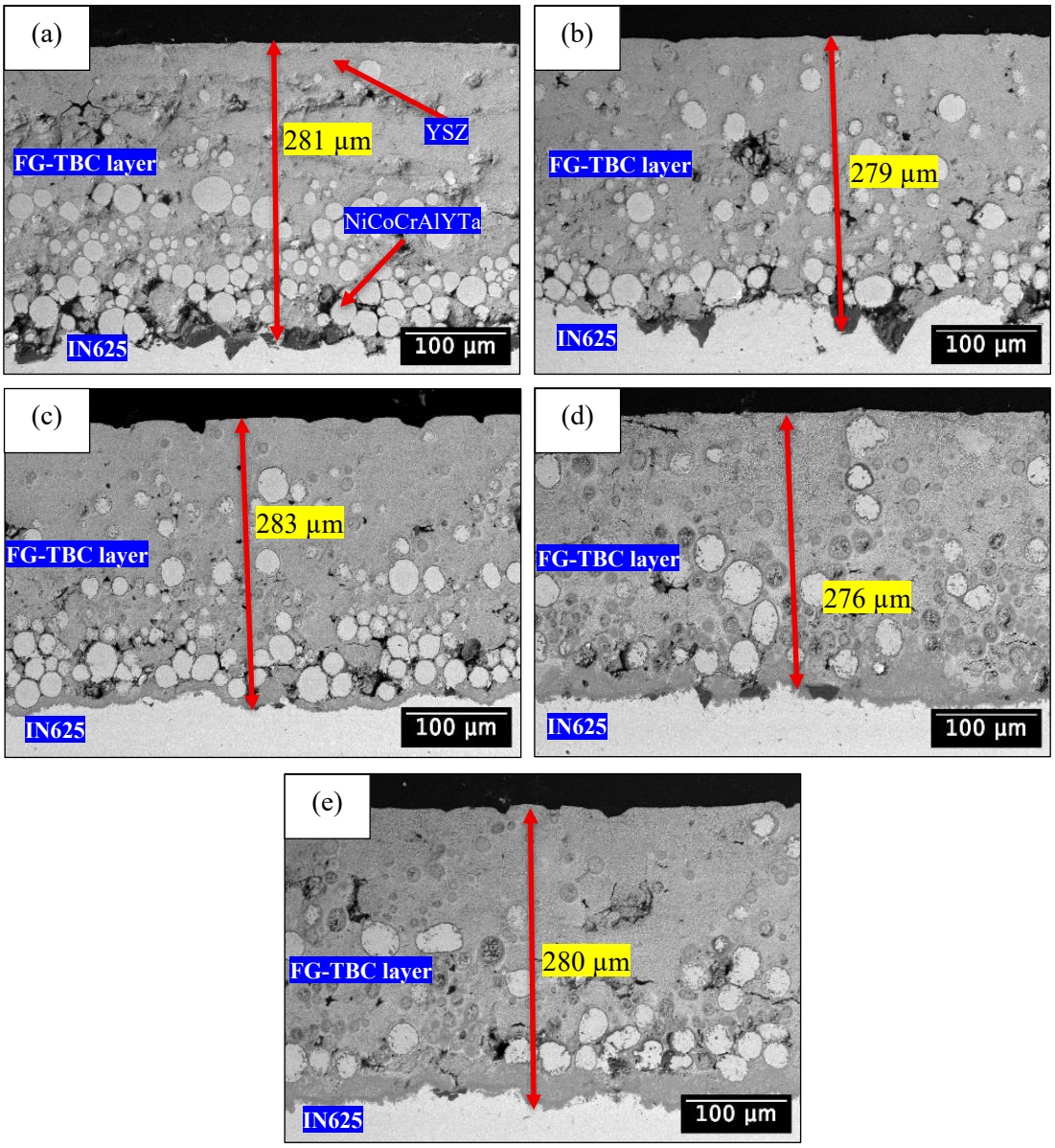

Figure 2: Cross-sectional microstructure of sample (a) S950, (b) S1000, (c) S1050, (d) S1100 and (e) S1150

Figure 3 displays cross-sectional microstructures of all coated samples at higher magnification, focusing on the metallic-rich layer near the substrate. A continuous reaction layer was observed in samples S1050, S1100, and S1150, whereas no reaction layer formed in samples S950 and S1000, suggesting that the thermal energy at these lower temperatures was insufficient to initiate interfacial reactions between the coating and the substrate. In addition, porosities were observed in samples S950, S1000, and S1050. Conceptually, SST involves spraying a suspension of solid particles in water onto a substrate at room temperature. Water trapped between particles or at the coating layer interfaces can leave behind pores as it evaporates. The porosities can also form during the debinding process, where voids were formed as the binder was burned out from the coating layers. These internal voids should be diminished during sintering, as the coatings densify due to volumetric shrinkage. Hypothetically, higher sintering temperature led to higher coating shrinkage, thereby reducing porosity [15]. According to this finding, shrinkage was considerably limited at temperatures lower than 1100 °C, thus resulting in poor

particle bonding. In contrast, Figure 3(e) shows the presence of cracks in sample S1150, indicating that the coating was over-sintered. Over-sintering can produce a brittle composite, induce additional stresses and increase micro-crack formation in the coating structure [16].

As the sintering temperature increased, tensile stresses localized near the substrate interface due to the restriction of volumetric shrinkage of the FG-TBC layer, which was constrained by the rigid substrate. Cracks were more likely to form because of limited volumetric shrinkage combined with thermal expansion mismatch between the coating layers and the substrate. Meanwhile, sample S1100 in Figure 3(d) depicts FG-TBC layers with minimal porosity, and no visible cracks were observed, signifying sufficient densification without an over-sintering effect. Other than sintering temperatures, the process of fabricating the green coating itself has influenced the microstructures. Porosity and crack formation in samples sintered at temperatures below and above 1100 °C can be reduced by controlling the drying environment and ensuring an inert atmosphere during sintering.

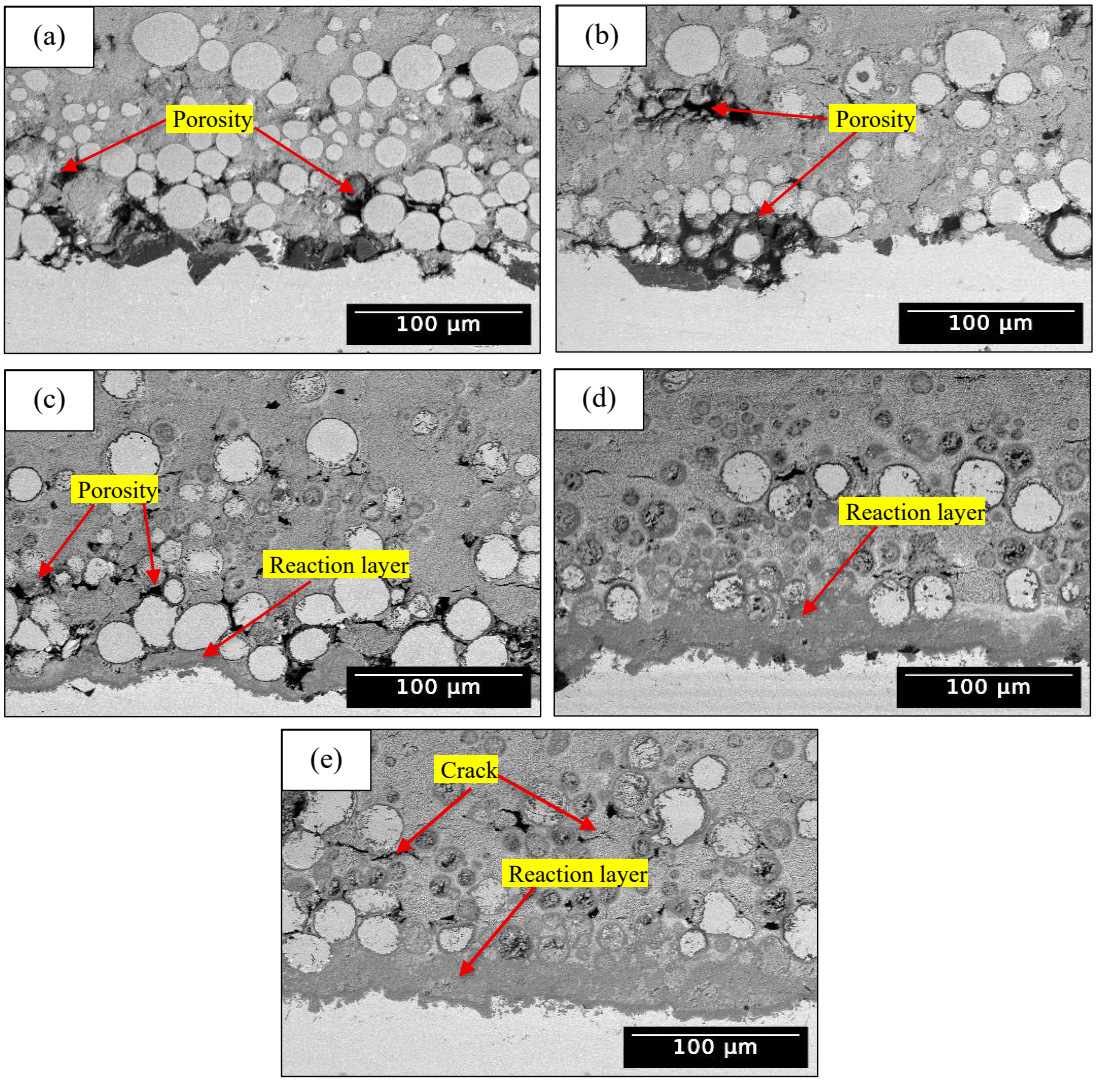

Figure 3: Cross-sectional microstructure of sample (a) S950, (b) S1000, (c) S1050, (d) S1100 and (e) S1150 at higher magnification

Figure 4 shows that the reaction layer thickness increases with sintering temperature, ranging from 12 ± 3 µm in S1050 to 56 ± 6 µm in S1150. The sample sintered at 1050 °C revealed the lowest thickness of the reaction layer (12 ± 3 µm), whereas the sample sintered at 1150 °C displayed the highest thickness (56 ± 6 µm). This finding was consistent with previous studies, which reported that higher sintering temperature promoted the formation and thickening of new reaction products at the coating-

substrate interface [17]. This phenomenon can be attributed to increased atomic mobility at elevated temperatures, which enhanced elemental diffusion across the interface. Besides, higher sintering temperature enhanced oxidation reaction, which accelerated the diffusion of oxygen into the coating layer and reacted with bond coat elements. According to the plasma spray technique, this reaction layer was commonly known as thermally grown oxide (TGO), which ideally consists of a continuous alumina (Al_2O_3) inner layer and a minimal mixed oxides (i.e., $NiCr_2O_4$, $(Ni, Co)(Cr, Al)_2O_4$) outer layer [18].

In contrary, EDX analysis (Figure 5) revealed a reaction zone dominated by mixed oxides with localized Al_2O_3 formation. Specifically, point A in Figure 4(b) corresponded to the thick outer layer of the reaction zone, identified as spinel $(Ni(Cr, Al)_2O_4)$ as proven in the EDX analysis in Figure 5(a), while EDX analysis in Figure 5(b) showed presence of chromia (Cr_2O_3) in the thin inner layer of the reaction zone as referred in point B in Figure 4(b). Previous research reported that at high temperatures, the diffusion coefficient of Cr is higher than that of Al, resulting in faster outward diffusion of Cr [19]. Therefore, the formation of Cr_2O_3 increases rapidly while impeding Al diffusion, thus leading to localized formation of Al_2O_3 even if sufficient Al is present in the bond coat particles. Compared to TBC deposited by APS or EB-PVD, slurry-sprayed coatings are less dense and exhibit high porosity, which facilitates high oxygen penetration through the coating layers and accelerates the formation of a thick mixed-oxide reaction layer.

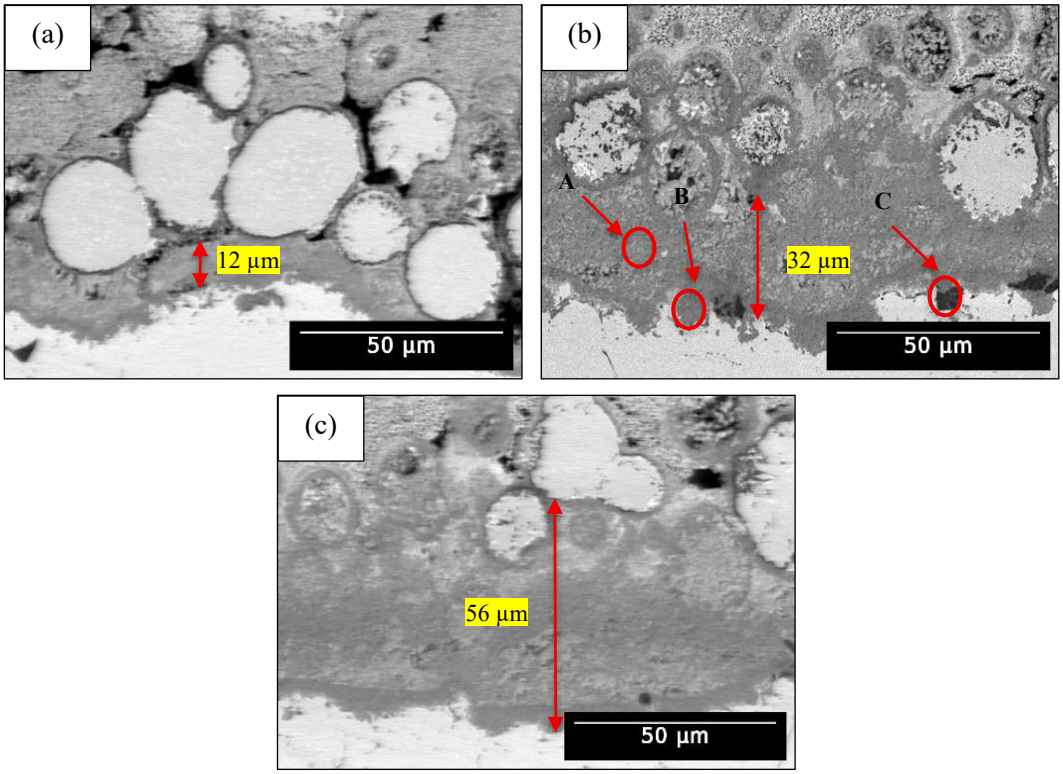

Figure 4: Reaction layer thickness for sample (a) S1050, (b) S1100 and (c) S1150

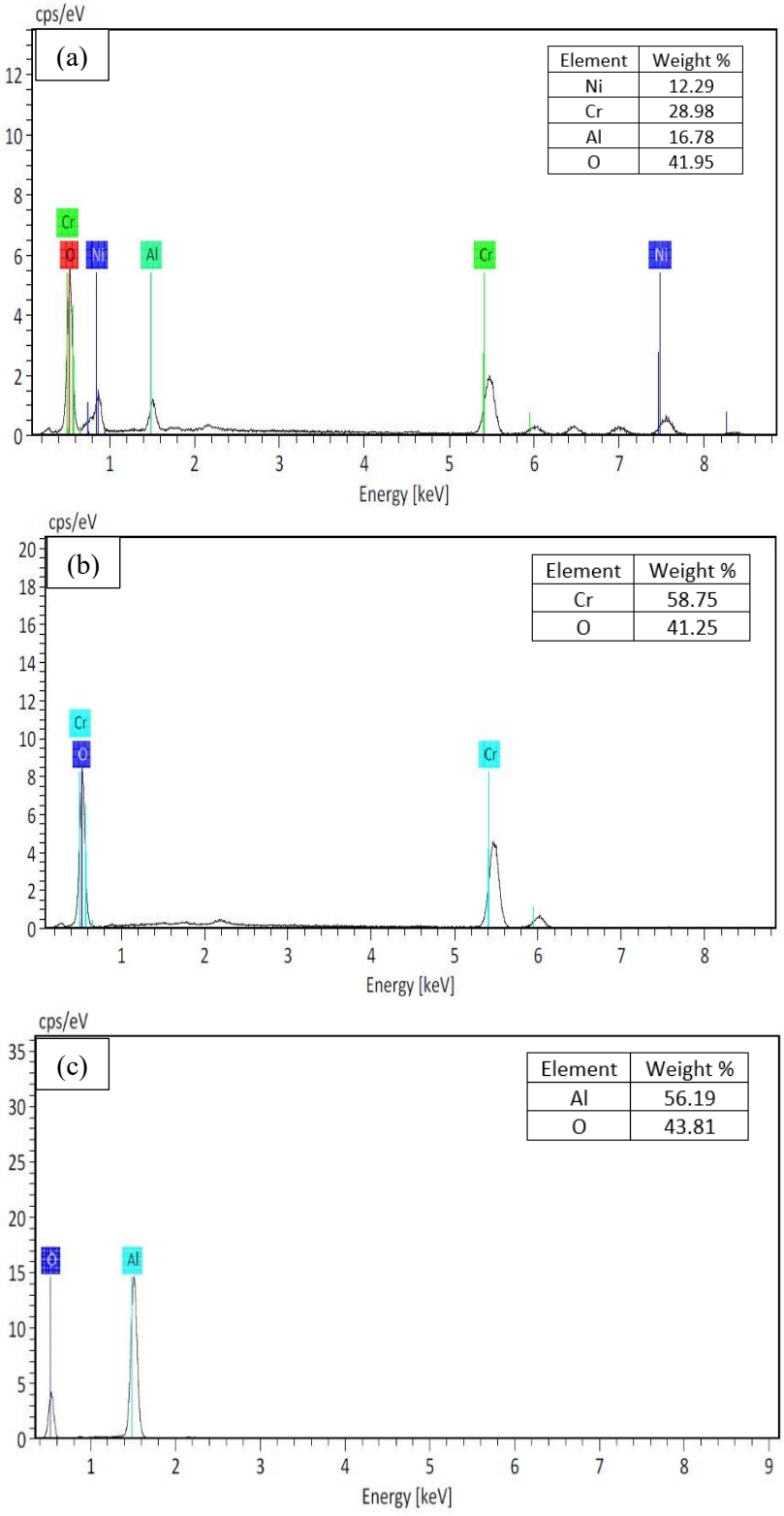

Figure 5: EDX analysis of points (a) A, (b) B, and (c) C in Figure 4(b)

3.2 Adhesion strength at various sintering temperatures

Figure 6 illustrates the average adhesion strength for all coated samples sintered at different temperatures. An ascending trend in adhesion strength was observed as the sintering temperature increased from 950 to 1100 ℃. However, the adhesion strength decreased as the sintering temperature

rose to 1150 ℃. Particularly, the sample sintered at 950 ℃ displayed the lowest adhesion strength of 10.23 ± 0.8 MPa, while the sample sintered at 1100 ℃ showed the highest adhesion strength of 22.87 ± 0.5 MPa. As the sintering temperature increased, particle bonding in the FG-TBC was enhanced, leading to lower porosity and greater densification. Consequently, mechanical interlocking between particles was strengthened, leading to improved bonding between coating layers and substrate. Adhesion strength of sample S1100 was higher than previous works of FG-TBC deposited by SST [12, 13]. However, at 1150 ℃, the adhesion strength decreased due to the formation of cracks within the coating layers, arising from high thermal stresses induced by thermal expansion mismatch between the coating and the substrate, which increased residual stresses in the FG-TBC. In addition, the thicker reaction layer was observed at this temperature, characterized by a high formation of mixed oxides, thus contributing to lower adhesion strength. This brittle interfacial layer diminished effective contact between coating and substrate, compromising adhesion strength and increasing the risk of coating spallation [20].

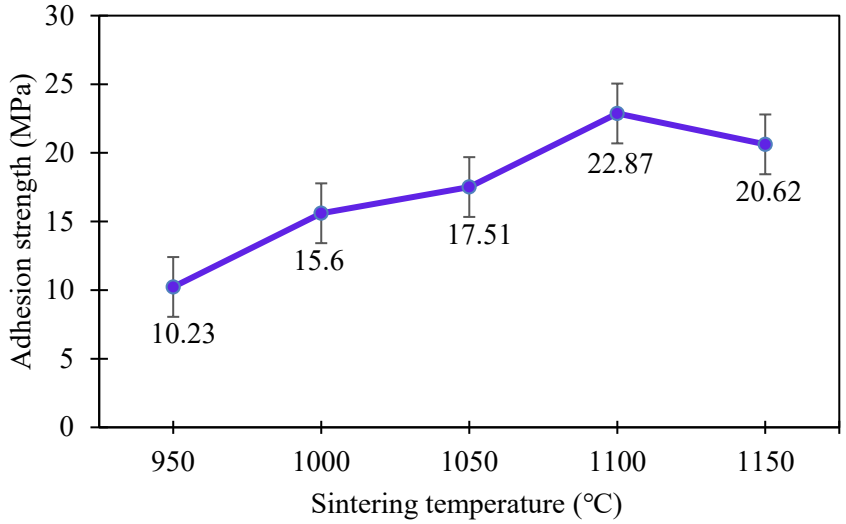

Figure 6: Adhesion strength of coated samples sintered at various sintering temperature

4. CONCLUSIONS

In this study, the three-layered YSZ/NiCoCrAlYTa FG-TBC was successfully deposited on Inconel 625 substrates using SST. In order to evaluate the feasibility of this TBC for gas turbine applications, several key parameters were investigated, with particular emphasis on the sintering temperature. A range of sintering temperatures from 950 to 1150 ℃ was selected for evaluation. Microstructural analysis and adhesion strength evaluation were conducted as preliminary assessments in determining the effective sintering temperature for slurry-sprayed YSZ/NiCoCrAlYTa FG-TBC. According to this study, cross-sectional microstructures showed consistent coating thickness for all samples with an average thickness of 280 µm, indicating good repeatability and stability during the slurry spray process. A continuous reaction layer was developed in samples S1050, S1100, and S1150, whereby an insignificant reaction layer was formed in samples S950 and S1000. Porosities were observed in samples S950, S1000, and S1050, whereas cracks were present in sample S1150. Sample S1100 revealed dense FG-TBC layers with minimal porosity and no presence of cracks. The reaction layer was rich in mixed oxides with localized Al_2O_3 formed at the substrate interface. The thickness of the reaction layer increased with increasing sintering temperature. Adhesion strength increased as sintering temperature increased from 950 ℃ to 1100 ℃ and started to decrease as sintering temperature rose to 1150 ℃. Sample S1100 showed the highest adhesion strength of 22.87 ± 0.5 MPa. The effective sintering temperature for YSZ/NiCoCrAlYTa FG-TBC was achieved at 1100 ℃.

Acknowledgements

The authors would like to acknowledge the financial support from the Ministry of Higher Education Malaysia and Research Management Center, Universiti Teknologi Malaysia under the projects R.K130000.7857.5F749 (FRGS/1/2024/TK10/UTM02/13), R.J130000.7724.4J64 (UTM R&D Fund), Contract Research R.J130000.7624.4C824 (Project), R.J130000.7624.4C823 (Program) and Q.J130000.3824.23H64 (UTM FR).

Author Contributions

All authors contributed toward data analysis, drafting and critically revising the paper and agree to be accountable for all aspects of the work.

Disclosure of Conflict of Interest

The authors have no disclosures to declare.

Compliance with Ethical Standards

The work is compliant with ethical standards.

References

[1] Salwan, G. K., Subbarao, R. & Mondal, S. (2021). Comparison and selection of suitable materials applicable for gas turbine blades. *Materials Today: Proceedings*. 46(17), 8864-8870.

[2] Swain, B., Mallick, P., Patel, S., Roshan, R., Mohapattra, S. S., Bhuyan, S., Priyadarshini, M., Behera, B., Samal, S. & Behera, B. (2020). Failure analysis and materials development of gas turbine blades. *Materials Today: Proceedings*, 33(8), 5143–5146.

[3] Liu, Q., Huang, S. & He, A. (2019). Composite ceramics thermal barrier coatings of yttria stabilized zirconia for aero-engines. *Journal of Materials Science & Technology*, 35(12), 2814-2823.

[4] Mehboob, G., Liu, M. J., Xu, T., Hussain, S. & Tahir, A. (2020). A review on failure mechanism of thermal barrier coatings and strategies to extend their lifetime. *Ceramics International*, 46(7), 8497-8521.

[5] Fathi, R., Wei, H., Saleh, B., Radhika, N., Jiang, J., Ma, A., Ahmed, M. H., Li, Q. & Ostrikov, K.K., (2022). Past and present of functionally graded coatings: Advancements and future challenges. *Applied Materials Today*, 26, 101373.

[6] Islam, A., Sharma, A., Singh, P., Pandit, N. & Keshri, A. K. (2022). Plasma-sprayed CeO_2 overlay on YSZ thermal barrier coating: Solution for resisting molten CMAS infiltration. *Ceramics International*, 48(10), 14587-14595.

[7] Yang, W. & Ye, F. (2021). The thermophysical properties and the molten CMAS resistance performance of Ytterbium Tantalate. *Surface and Coatings Technology*, 423, 127584.

[8] Kumar, V. & Balasubramanian, K. (2016). Progress update on failure mechanisms of advanced thermal barrier coatings: a review. *Progress in Organic Coatings*, 90, 54-82.

[9] Curry, N., VanEvery, K., Snyder, T. & Markocsan, N. (2014). Thermal conductivity analysis and lifetime testing of suspension plasma-sprayed thermal barrier coatings. *Coatings,* 4(3), 630–650.

[10] Zou, Z., Donoghue, J., Curry, N., Yang, L., Guo, F., Nylen, P., Zhao, X. & Xiao, P. (2015). A comparative study on the performance of suspension plasma sprayed thermal barrier coatings with different bond coat systems. *Surface and Coating Technology*, 275, 276–282.

[11] Naseem, M., Verma, R. & Kango, S. (2020). Thermo-mechanical evaluation of slurry-sprayed multi-layered coatings. *Arabian Journal for Science and Engineering,* 45(11), 9449–9470.

[12] Verma, R., Randhawa, J. S., Kant, S. & Suri, N. M. (2019). Characterization studies of slurry-sprayed mullite–nickel coatings on ASTM 1018 steel. *Arabian Journal for Science and Engineering*, 44(6), 5897–5919.

[13] Nguyen, P., Ho, S. Y. & Kotousov, A. (2013). Slurry spray technique for manufacturing thermal barrier coatings. *Surface Innovations*, 1(3), 190–199.

[14] Nguyen, M. D., Bang, J. W., Kim, Y. H., Bin, A. S., Hwang, K. H., Pham, V. H. & Kwon, W. T. (2018). Slurry spray coating of carbon steel for use in oxidizing and humid environments. *Ceramic International,* 44(7), 8306–8313.

[15] Jiang, C., Li, R., He, F., Cheng, Z., Li, W. & Zhao, Y. (2024). Anti-sintering behavior of GYYSZ, thermophysical properties, and thermal shock behavior of thermal barrier coating with YSZ/Composite/GYYSZ system by atmospheric plasma spraying. *Nanomaterials,* 14(22), 1787.

[16] Xiao, K., Xue, W., Li, Z., Wang, J., Li, X., Dong, C., Wu, J., Li, X. & Wei, D. (2018). Effect of sintering temperature on the microstructure and performance of a ceramic coating obtained by the slurry method. *Ceramic International*, 44(10), 11180–11186.

[17] Dudina, D. V., Kvashnin, V. I., Bokhonov, B. B., Legan, M. A., Novoselov, A. N., Bespalko, Y. N., Jorge Jr, A. M., Koga, G. Y., Ukhina, A. V., Shtertser, A. A. & Anisimov, A. G. (2023). Metallic iron or a Fe-based glassy alloy to reinforce aluminum: reactions at the interface during spark plasma sintering and mechanical properties of the composites. *Journal of Composites Science*, 7(7), 302.

[18] Ding, K., Zhang, T., Wang, Z., Yu, J., Guo, W. & Yang, Y. (2022). Effect of thermal growth oxide composition and morphology on local stresses in thermal barrier coatings. *Materials*, 15(23), 8442.

[19] Shi, G., Zhang, L. & Wang, Z. (2020). Modelling the elements reaction–diffusion behavior on interface of Ti/Al2O3 composite prepared by hot pressing sintering, *Metals*, 10(2), 259.

[20] Boissonnet, G., Grégoire, B., Bonnet, G. & Pedraza, F. (2019). Development of thermal barrier coating systems from Al microparticles. Part I: Influence of processing conditions on the mechanisms of formation. *Surface and Coatings Technology,* 380, 125085.